Analytical Methods

Accepted Manuscript

This article can be cited before page numbers have been issued, to do this please use: J. Zhao, S. Fang, L. Zeng, Z. He and Y. Liu, *Anal. Methods*, 2020, DOI: 10.1039/D0AY01137A.

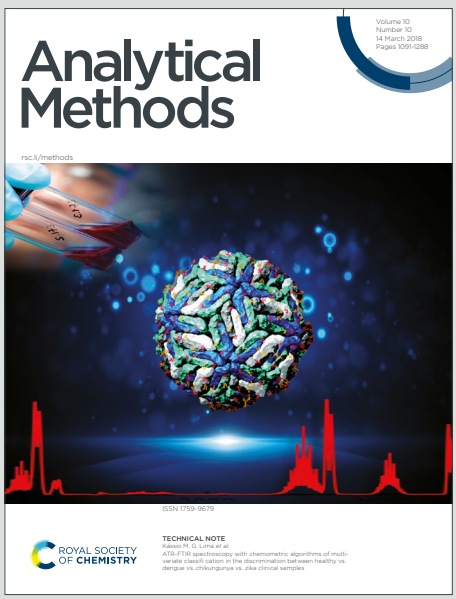

ROYAL SOCIETY OF CHEMISTRY

rsc.li/methods

View Article Online
DOI: 10.1039/D0AY01137A

ARTICLE

A lateral flow biosensor based on gold nanoparticles detects four hemorrhagic fever viruses

Received 00th January 20xx,
Accepted 00th January 20xx

DOI: 10.1039/x0xx00000x

Jin Zhao[a], Shuting Fang[b], Yujie Liu[a], Lingwen Zeng,*[,b,c], Zhixu He*, [a]

Abstract: The pathogen of a viral hemorrhagic fever (VHF), which is harmful to human health, is a hemorrhagic fever virus. Clinicians have long needed convenient and sensitive point-of-care rapid diagnostic tests (RDTs) for hemorrhagic fever virus. Commonly used methods for pathogen detection rely on conventional culture-based tests, antibody-based assays and polymerase chain reaction (PCR)-based techniques. However, these methods are costly, laborious and time-consuming. Herein, we present a simple and sensitive biosensor for the rapid detection of hemorrhagic fever virus. For this assay, we develop lateral flow biosensors (LFBs) based on magnetic beards and nicking enzyme-assisted isothermal strand-displacement amplification (SDA) for the detection of hemorrhagic fever virus. The detection limit of this assay is 10 fM.

Keywords RDTs; LFBs; SDA; hemorrhagic fever viruses

Introduction

A hemorrhagic fever virus is the pathogen of a viral hemorrhagic fever (VHF), and such fevers destroy the vascular system of the body and homeostasis and then cause fever, malaise, bleeding abnormalities, neurological disorders and circulatory shock with high mortality[1-3]. Hemorrhagic fever virus, which has strong toxicity and high infectivity, is divided into four RNA virus families: *Arenaviridae*, *Filoviridae*, *Bunyaviridae* and *Flaviviridae*[4-6]. The clinical symptoms caused by hemorrhagic fever virus are not very specific and thus need to be differentiated from those of hemorrhagic fever caused by different viruses[7-10]. The more common pathogens are yellow fever virus, dengue virus (DENV) and Ebola virus (EBOV)[11]. In terms of geographic distribution, DENV is found mainly in southern China[12], hantavirus (HTNV) is mainly observed in northeastern China[13], and Ebola hemorrhagic fever (EHF) in humans has been reported in central Africa[14]. Hemorrhagic fever virus pathogens are mainly transmitted by infected animals, insect hosts or patients in the acute phase, most of which are rodents and arthropods[4, 15-16], such as ticks and mosquitoes[17-20]. The outbreak of the EBOV in 2014 led to more than 7000 deaths, with a mortality rate of over 50%[21]. In the same year, the outbreak of dengue infection in Guangdong Province affected over 40,000 people[22]. Furthermore, a definitive diagnosis of VHF relies mainly on laboratory testing.

The current methods for the detection of hemorrhagic fever virus are divided into the following four categories. (a) Isolation and culture. The virus is inoculated onto cell cultures to isolate the virus. One to two weeks after inoculation, cells infected with the virus can be identified using immunofluorescence. Isolation is laborious and time consuming, and there is involves a high risk of viral contamination in the laboratory; thus, biosecurity measures are required to protect the handler from exposure to aerosols[23]. (b) Polymerase chain reaction (PCR). PCR enables the rapid and highly efficient detection of the conserved sequences in the genome of a virus with high specificity[24]. (c) Enzyme-linked immunosorbent assay (ELISA). For ELISA, the most commonly

[a.] *Guizhou Provincial Key Laboratory for Regenerative Medicine, Tissue Engineering and Stem Cell Research Center, Depart-ment of Immunology, School of Basic Medical Science, Guizhou Medical University, Guiyang 550004, China*
[b.] *School of Food Science and Engineering, Foshan University, Foshan 528231, China.*
[c.] *Key Laboratory of Regenerative Biology, South China Institute for Stem Cell Biology and Regenerative Medicine, Guang-zhou Institutes of Biomedicine and Health, Chinese Academy of Sciences, Guangzhou 510530, China.*
* Corresponding Author
Lingwen Zeng, zeng6@yahoo.com; Zhixu He, hzx@gmc.edu.cn

used method, the detection sensitivity is high, but sampling poses an infection risk[25]. (d) Lateral flow biosensor. Such devices are convenient, fast, and suitable for on-site detection, and they have higher specificity and sensitivity than ELISA[24, 26]. In recent years, multiple real-time quantitative PCR detection techniques and DNA microarray assays with high sensitivity and good specificity have been developed[27-28]. However, skilled technicians are required to operate the complex instruments. Therefore, there is an urgent need for a simple, rapid, sensitive and accurate detection method for hemorrhagic fever virus.

To improve the sensitivity of sensors, considerable attention has been paid to DNA-based amplification methods, such as PCR, rolling circle amplification, exonuclease signal amplification, nicking endonuclease signal amplification, and strand displacement amplification (SDA). SDA is a common method of isothermal amplification. In 1992, Walker proposed a DNA amplification technique for developing the strand-displacement polymerization reaction[29]. In 2009, Guo proposed the isothermal strand-displacement polymerization reaction, which is a simple detection technique based on the strand-displacement polymerization reaction[30]. The isothermal strand-displacement polymerization reaction is a nucleic acid isothermal amplification technique based on the enzymatic reaction of a polymerase and a cleavage enzyme. The nucleic acid sequence is amplified by using the cleavage enzyme at the recognition site and the ability of the polymerase to extend and replace the downstream sequence at the incision site. In this study, we developed a lateral flow biosensor (LFB) based on SDA for the simple and rapid detection of DENV and HTNV, and it is also suitable for other kinds of hemorrhagic fever viruses such as chikungunya fever virus (CHIKV) and EBOV (Figure 1).

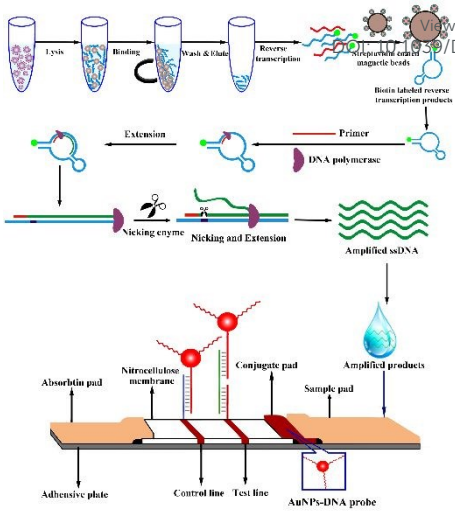

Figure. 1 Scheme of an LFB based on SDA for hemorrhagic fever virus detection. The amplified product is loaded onto the sample pad for visual detection.

Results and discussion

Design of probes for the detection of four kinds of hemorrhagic fever virus

The universal primers were designed by based onblasting at least subtype sequences of each hemorrhagic fever virus throug NCBI. After blasted all subtype sequences, the specific primers were designed according its highly conserved sequences of each kind hemorrhagic fever virus. The capture-probe was modified with biotin for magnetic separation. A primer sequence and an Nb.BbvCI recognition site were added at the 3' end of the capture-probe for SDA. The AuNP-probe was modified with a thiol group at the 5' end for AuNP coating. The T-line and AuNP-probe complement the two fragments of the amplified target, thereby forming a sandwich link between the test zone and AuNPs. The C-line is a DNA sequence complementary to the AuNP-probe (Table 1-4).

View Article Online
DOI: 10.1039/D0AY01137A

Table 1. HTNV oligonucleotide sequences [a,b,c,d,e]

HTNV oligonucleotide	Sequence 5'-3'
Capture-probe	B-n-ACAGCCTCCTTTCCCCAGGCAACCATGAAGAGCACAATAATTCGCTGAGG**CTAGTTGTATCCCCAT**
Primer	ATGGGGATACAACTAGGCCAGAATGGGGATACAACTAGGCCAGA
Control-probe	TCCCCTAAGTGGAAGTTGTCCTCCCCTAAGTGGAAGTTGTCC
AuNP-probe	S-n-GGACAACTTCCACTTAGGGGA
Forward primer	CCTACCTCAGAAGGACACAATCA
Reverse primer	CTGTGCCAGTGTCCTTAGCTC

Table 2. CHIKV oligonucleotide sequences

CHIKV oligonucleotide	Sequence 5'-3'
Capture-probe	B-n-CCCGGTCTGTTGACTAGAGTCTTATACGGTACTCCCACCGTGTGCTGAGG**TCACTGTTACGTGT**
Primer	ACACGTAACAGTGATCCCGAACACGTAACAGTGATCCCGA
Control-probe	CCAGTACCATGGGGCTGTAGCCAGTACCATGGGGCTGTAG
AuNP-probe	S-n-CTACAGCCCCATGGTACTGG
Forward primer	ACTGTGAGCGCGTACGAA
Reverse primer	AGTGACTGACAGTAGCTCCATC

Table 3. DENV oligonucleotide sequences

DENV oligonucleotide	Sequence 5'-3'
Capture-probe	B-n-GAAAAAGGCGAAAAACACGCCTTTCAATATGCTGAGG**TTATTCACAGAGATCTGC**
Primer	GCAGATCTCTGATGAATAACCAACGGCAGATCTCTGATGAATAACCAACG
Control-probe	GGTTTCTCTCGCGTTTCAGCGGTTTCTCTCGCGTTTCAGC
AuNP-probe	S-n-GCTGAAACGCGAGAGAAACC
Forward primer	AGCTCAACGTAGTTCTAACAGTTT
Reverse primer	TGTTGCACAGTCGACACG

Table 4. EBOV oligonucleotide sequences

EBOV oligonucleotide	Sequence 5'-3'
Capture-probe	B-n-TATTGTATCAGTCCTTGCTCTGCATGTACTTGAATTTGCCTTTGAGCTGAGG**TCAAGGCAAGCCTTT**
Primer	AAAGGCTTGCCTTGAGAAGGTAAAGGCTTGCCTTGAGAAGGT
Control-probe	ACTGATTGCCAAGCTGTTGGAACTGATTGCCAAGCTGTTGGA

View Article Online
DOI: 10.1039/D0AY01137A

AuNP-probe	S-n-TCCAACAGCTTGGCAATCAGT
Forward primer	CCTTCCGAAATTGGTAGTAGGAG
Reverse primer	ACGGAAAATCACCATCATGTGTC

a Underlined letters indicate the recognition sequence of Nb.BbvCI.

b Bold letters indicate the additional primer sequence.

c B indicates a 5' biotin modification.

d n Indicates a C9 linker.

e S indicates a 5' thiol modification.

Published on 02 October 2020. Downloaded on 10/5/2020 11:01:07 PM.

Preparation and optimization of the materials for AuNPs-based LFBs

AuNPs were prepared using the trisodium citrate reduction method and measured using a Cary 100 UV spectrophotometer. The maximum absorption peak of the AuNPs was 523 nm, indicating that the diameter of AuNP was approximately 15 nm (Figure 2a). Then, the concentrated AuNPs were evenly sprayed on fiberglass paper; the optimal amount of AuNPs was 4 μL / cm (Figure 2b). Next, 10 μL of the SDA product was diluted to 50 μL with sample loading buffer containing 4 × sodium citrate and 0.1% Triton X-100, and it could achieve good flowability (Figure 2c). Thus, the optimization of the construction of the LFBs was preliminarily completed. Furthermore, to determine the best SDA reaction time, SDA reaction systems were amplified for 10, 20, 30, 60 or 90 min, and the ratio of the amplification signal to the background signal (signal-to-noise ratio) showed that the best amplification reaction time was 30 min (Figure 2d).

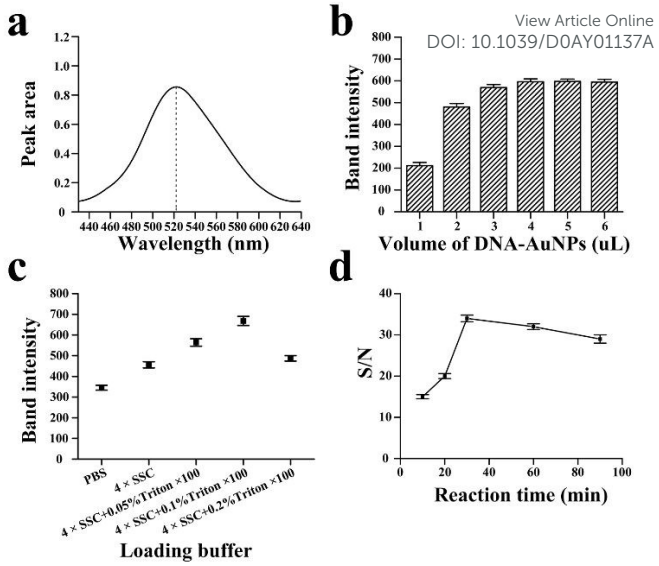

Figure 2. Optimization conditions of the materials for AuNPs-based LFBs. a. Optimization of AuNPs; b. Optimization of the volume of AuNPs; c. Optimization of sample loading buffer; d. Optimization of SDA reaction time.

Specificity analysis of LFBs for the detection of four kinds of hemorrhagic fever virus

The SDA reaction template for DENV was obtained from C6/36 cells (infected with DENV-2) and culture medium, and caused the safety concerns, for those of HTNV, CHIKV and EBOV, 10^4 fM recombinant virus plasmid was used as the templates instead of real samples. 20 μL ssDNA samples of the SDA reaction products of HTNV, DENV, CHIKV and EBOV were loaded onto separate LBFs (Figure 3a shows the specificity analysis for HTNV). The band on test line clearly shows that this biosensor works for hemorrhagic fever virus detection, and no cross detection showed in this assay (Figure 3a). Only target virus ssDNA produced a red line, and other ssDNA samples did not produce a visible test line. These results demonstrated the high specificity of the current biosensor. To further explored the biosensor could be used for four individual kinds of hemorrhagic fever virus detection , we used 10^4 fM of four kinds of virus recombinant plasmid. The band intensity results showed that each kinds of virus could be detected by using this biosensor(Figure 3b).

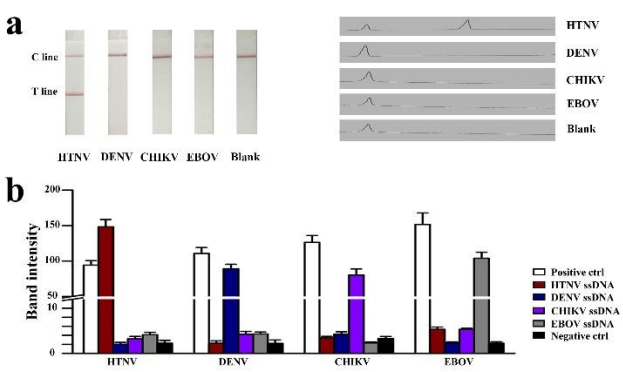

Figure 3. Selectivity of the biosensors. a. Typical images of the LFBs for the detection of HTNV. The images from left to right show the detection of all four stains of hemorrhagic fever virus ssDNA, i.e., HTNV, DENV, CHIKV, and EBOV, as well as normal human serum as a negative control (left). The photo was taken within 20 minutes of sample loading. The band intensity curve (right). b. Positive control was performed with 10^4 fM of four kinds of virus recombinant plasmid; the bar graph shows the selectivity for each virus biosensor (from left to right: HTNV, DENV, CHIKV, and EBOV), and the band intensity was analyzed using Quantity One software (n=6). *p< 0.05 vs. negative control.

The SDA reaction for the detection of the four kinds of hemorrhagic fever virus

The sensitivity of the SDA reaction was examined by using plasmid samples at different concentrations. First, the plasmid samples were dissolved in water at the following six concentrations: 10^{12} fM, 10^8 fM, 10^6 fM, 10^4 fM, 10^2 fM, 10 fM and 0 (blank control). For each test, virus plasmid samples of different concentrations were added to 20 μL of SDA reaction solution. The amplification products were analyzed using a 2% agarose gel at a 100 V constant voltage for 30 min. Fig. 2 shows that, when the concentration of each plasmid sample increases from 10 fM to 10^{12} fM, the band intensity of the amplification product increases correspondingly (Figure 4a, b).

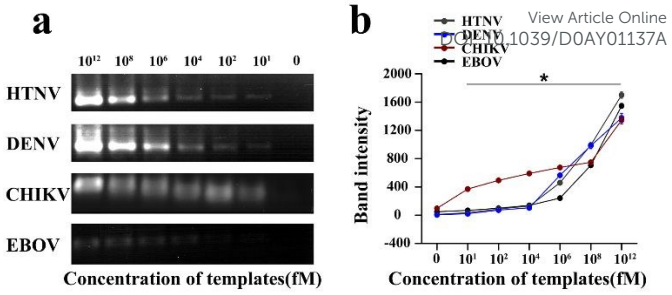

Figure 4. 2% agarose gel electrophoresis analysis of the SDA method. a. From left to right, the concentrations of each plasmid samples are 10^{12} fM, 10^8 fM, 10^6 fM, 10^4 fM, 10^2 fM, 10^1 fM, and 0 fM (water). b. The band intensity of the amplification products was analyzed using Quantity One software (n=6). *p<0.05 vs. 0 fM.

The comparison of SDA with PCR

In order to demonstrated sensitivity of SDA amplification, we used the same templates and the same primers by using PCR method. The PCR results showed that, the universal primers in SDA system was also able to be used in PCR systems with highly sensitivity(Figure 5 a, b). We then compared the band intensity of two DNA amplification, which showed no significant difference between two method, indicated that SDA could stably amplify the target DNA(Figure 5c,d).

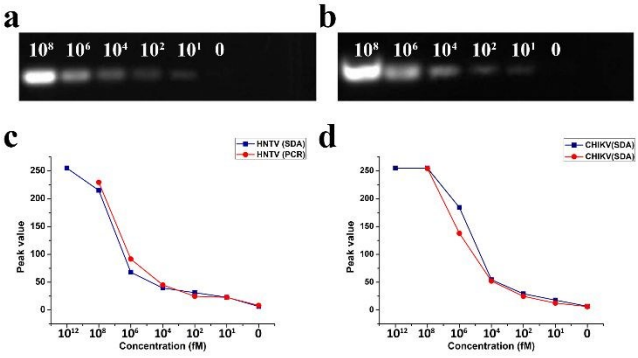

Figure 5. Sensitivity analysis comparison between SDA reaction and PCR results. a and b， 2% agarose gel electrophoresis analysis of the PCR method. From left to right, the concentrations of each plasmid samples are 10^8 fM, 10^6 fM, 10^4 fM, 10^2 fM, 10^1 fM, and 0 fM (PBS) ； (a) HNTV, (b) CHIKV ； c, d, Band strength analysis of SDA amplification products compared with PCR amplification products.

View Article Online
DOI: 10.1039/D0AY01137A

Sensitivity of the LFBs for four kinds of hemorrhagic fever virus detection

The sensitivity of the LFBs was examined by using four kinds of hemorrhagic fever virus plasmid samples at different concentrations. From left to right, the concentrations of the plasmid samples were 10^{12} fM, 10^{6} fM, 10^{4} fM, 10^{2} fM, 10^{1} fM and 0 fM (negative control, loading buffer). For each test, different concentrations of each virus plasmid sample were loaded on LFBs. The optical intensities of the red bands on the test zones increased with the increase in HTNV plasmid sample concentration, and no red band was observed on the test zone in the absence of plasmid sample (negative control, 0 fM) (Figure 6a). Furthermore, it was easy to distinguish the presence of the red band after adding 10^{1} fM plasmid samples from the absence of the red band after adding 0 fM plasmid samples on the test zone with the naked eye. Therefore, the limit of detection (LOD) for visual detection was set to 10^{1} fM by analyzing band intensity (Figure 6c). The calibration curves in Fig. 6b (inset) showed that the optical intensities of the red bands are proportional to the logarithm of the plasmid sample concentration in the range from 10^{1} fM to 10^{12} fM and that the linear correlation coefficients of the optical intensities of the red bands plotted as a function of the concentration of each plasmid sample (HTNV, DENV, CHIKV and EBOV) were above 0.9485, 0.9826, 0.8172, and 0.9011, respectively.

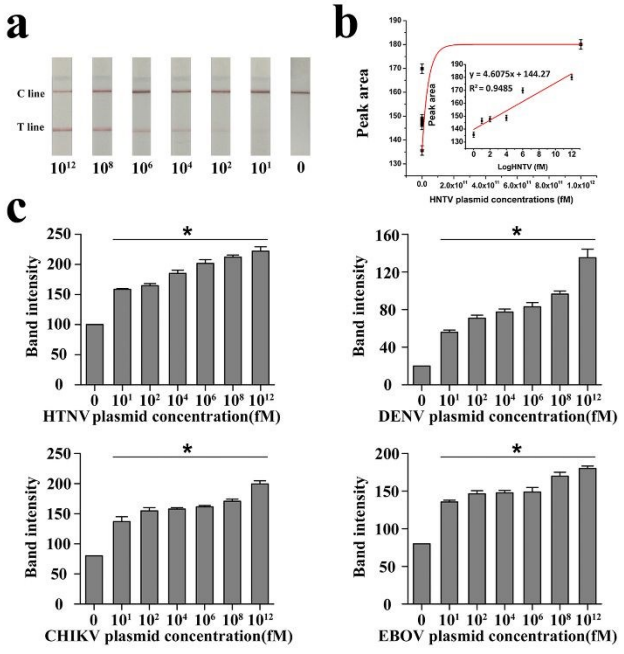

Figure 6. Typical images of the biosensors for the detection of HTNV virus plasmid samples. a. From left to right, the concentrations of each plasmid sample are 10^{12} fM, 10^{6} fM, 10^{4} fM, 10^{2} fM, 10^{1} fM, and 0 fM. b. Plots of the optical intensities of the red bands on the test zone vs. plasmid samples of different concentrations. Inset: calibration curve of the optical intensities of red bands on the test zone vs. the log value of the plasmid sample concentration. The error bars represent the standard deviation of three independent measurements. c. The corresponding optical intensities of the strip biosensor in the presence of plasmid samples of different concentrations. *p< 0.05 vs. 0 fM.

Although several novel and promising methods, such as PCR-based methods, have been developed for hemorrhagic fever virus detection in foods and other types of samples, specialized equipment and highly trained personnel are still required. Thus, a point-of-care device, with a simple handling method, a reduced need for laboratory instruments, and a short assay time, emerges as an attractive in-field test. The ligated DNA products could be immobilized onto the test zone of the LFBs to form a red band that can be unambiguously interpreted by the naked eye.

SDA can extend specially hybridized DNA primers onto DNA templates while displacing downstream chains and recycling those displaced strands[32]. This amplification method requires simple instruments such as a water bath or an incubator and produces a large amount of nucleic acid products within 30 min with the assistance of the cutting enzyme. Furthermore, SDA increases the sensitivity of sensors for DNA more than PCR-based methods[33], and it increases the sensitivity of the sensors for RNA[34-35]. The limitations of conventional DNA amplification-based methods, such as high false-positive rates, can be largely reduced. In our study, the amplified products obtained by the SDA method were analyzed by gel electrophoresis, and the LOD could reach 10 fmol /L. Thus, with reduced handling and simpler equipment, this assay provided a simple and rapid alternative to conventional methods. Furthermore, tedious DNA extraction and purification steps were avoided with this SDA-based isothermal amplification method.

The membrane-based lateral flow immunochromatographic strip is a fast, low-cost and effective tool for rapid detection[36-38]. The first

View Article Online
DOI: 10.1039/D0AY01137A

commercial strip was used for hCG detection[39]; since then, various LFB products have been made commercially available for detection in different fields, such as biomedical diagnostics, drug detection, food safety and environmental monitoring[40-44]. AuNPs are the most common nanomaterial used as signal probes in LFBs, with spherical AuNPs ranging from 20 nm to 30 nm in diameter. AuNPs are easy to synthesize and operate and have good biocompatibility. These nanoparticles have a strong red color, and they can be observed by the naked eye or through the use of color readers to achieve better detection limits. In our assay, SDA-amplified products coated with AuNP were used as the capture probes in SDA-based LFBs. The combined use of the SDA method and LFBs improved the sensitivity, and the linearity, repeatability and stability of the results were good.

Experimental

Reagents and chemicals

Vent (exo-) DNA polymerase, Nb.BbvCI, and deoxynucleoside triphosphates (dNTPs) were purchased from New England Biolabs (New England, USA). Oligonucleotides were purchased from Shanghai Generay Biotech (Shanghai, China). $HAuCl_4$, streptavidin (SA), anti-streptavidin antibody produced in rabbit whole antiserum (anti-SA mAb) and bovine serum albumin (BSA) were obtained from Sigma-Aldrich (Steinheim, Germany). Tris-base, boric acid, ethylenediaminetetracetic acid (EDTA), and Triton X-100 were purchased from Guangzhou WhiGa Technology Ltd. (Guangzhou, China). FBS and RPMI 1640 medium were purchased from Gibco (Waltham, CA, USA). Nitrocellulose membrane was purchased from Sartorius (Goettingen, Germany). Absorbent paper, laminated cards and fiberglass were purchased from Shanghai Kinbio (Shanghai, China). All buffer solutions used in this study were prepared in our lab. Other chemicals were purchased from standard commercial sources and were of analytical grade purity. All the water used in this study was ultra-pure water (18.2 MΩ/cm, Millipore, Billerica, MA, USA).

Cells, viruses

An *Aedes albopictus* cell line, C6/36 cells were purchased from Shanghai Biotechnology company (Shanghai, China), and were cultured in RPMI 1640 medium with 10% FBS. For virus infection process, cells were performed in RPMI 1640 medium with 5% FBS. The dengue virus type 2 stain for C3/36 cells infection were kept in Immunology department of Guizhou Medical University.

Preparation of gold-nanoparticle (AuNP)–DNA conjugates

AuNPs (average size of 15 nm) were prepared according to our previously reported method[31]. Briefly, 0.0001% AuNPs (1 gram of AuNPs powder was dissolved in 10 mL water, and added 1 mL AuNPs solution in 100 mL water) were prepared and stored at 4 °C until use. AuNP–DNA conjugates was prepared according to our previously report method[31]. Next, 100 µL of 1 OD thiolated DNA was added to 1 mL of the AuNP solution, concentrated the AuNP solution 4 times in the centrifuge at 4 °C for 10 min each time, and shaken gently overnight at 4 °C. DNA-coated AuNPs (1.1 mL) were aged for 12 hours, then DNA-coated AuNPs were centrifuged at 10,000 g for 20 min at 4 °C and rinsed 3 times using rinsing buffer to remove any unbound DNA. Finally, red pellet suspension was dissolved in 150 µL of rinsing buffer and loaded onto fiberglass as a conjugate pad.

Construction of the LFBs

Thirty microliters of 100 µM DNA probes (test line probe and control line probe) were simultaneously dispensed onto the nitrocellulose membrane with a lateral flow dispenser (Shanghai Kinbio, Shanghai, China). The membrane was then dried at room temperature for 12 h. After being soaked in sample pad buffer (0.5% Triton, 1% BSA, 1% sucrose, 50 mM boric acid, pH 8.0), fiberglass was used as the sample pads; it was dried and stored at low humidity at room temperature. The sample pad, conjugate pad, nitrocellulose membrane and absorbent pad were attached along the long axis of an adhesive plate with an overlap of 1–2 mm and cut into 4-mm-wide strips using a paper cutter (Figure 1).

Construction of recombinant plasmid samples

The nucleotide sequences of 3 virus strains of each subtype of HTNV (segment S, NCBI GenBank M14626.1), CHIKV (CHIKVgp2, NCBI GenBank NC_004162.2), DENV (NS1, NCBI GenBank M29095.1), and EBOV (NP, NCBI GenBank NC_002549.1) were retrieved from GenBank and aligned using Vector NTI (version 11.0) sequence alignment software. All virus fragments were cloned on the pBluescript II SK (-) vector and transformed into E. coli competent cells. The E. coli competent cells were cultured aerobically for 16 h at 37 °C in 10 mL of Luria-Bertani (LB) medium (final OD>1 for each sample). The plasma was extracted by a plasmid extraction kit

(Tiangen, Beijing, China) and then stored in a refrigerator at −4 °C until use.

Extraction and reverse transcription of total RNA of virus by magnetic beads purification

Total RNA of DENV was extracted from the C6/36 cells and purified using magnetic bead technology. For RNA lysis and binding, lysis buffer, binding buffer and magnetic beads were mixed together before use. To form the C6/36 cells and virus pellets in cell culture medium, 500 µL of cell suspension was centrifuged at 4 °C and 14,000 g for 10 min; then, the supernatant was discarded. Next, 200 µL of lysis buffer containing magnetic beads was added, and the tube was vortexed for 10 min at room temperature. Then, the tubes were placed in a magnet tube holder, the supernatant was discarded and the RNA-bound beads were washed twice to remove unwanted substances. Finally, 60 µL of elution buffer was mixed with the RNA-bound beads to release total RNA from the surface of the beads.

The RNA was reverse transcribed into cDNA by using a PrimeScriptTM RT Reagent Kit with gDNA Erase (Takara, Beijing, China) according to the manufacturer's recommendations. The reverse transcription products were prelabeled with a biotin moiety, which was captured by streptavidin-coated magnetic beads for enrichment. Then, streptavidin-coated magnetic beads were added to the mixture. After three magnetic washing steps, reverse transcription products were used as a template for single-direction SDA.

Preparation of SDA reaction products for LFBs

Previously prepared reverse transcription products of each virus (1 µL) were added to 20 µL of reaction solution (1 µM primer S1 and S2, 0.1 µM primer B1 and B2, 1 U Nb.BbvCI, 5 U polymerase Klenow fragment exo-, 50 µM dNTPs, and 1 × polymerase Klenow fragment exo- reaction buffer). The resulting solution was incubated at 37 °C for 60 min. After amplification, 10 µL of the product was diluted in 50 µL of 4× saline-sodium citrate (SSC), 0.1% Triton X-100, and loaded onto the sample pad in the biosensor. The test line and control line of the biosensor were visually determined in 5 min. Thus, a reliable, point-of-care rapid diagnostic test (RDT) for pathogen diagnosis was established (Figure 1).

Data analysis

Dose-response curve fitting and data analysis were performed using linear regression analysis with Origin Pro software (version 17.0, Hampton, Massachusetts, USA). Each result is presented as the mean ± SD. To detect statistical correlations, Spearman's rank correlation coefficient (R^2) was calculated between the optical intensities of red bands on the test zone and the log value of each plasmid sample concentration.

Conclusions

In conclusion, we developed a lateral flow biosensor (LFB) based on strand displacement amplification (SDA) for the simple and sensitive detection of four kinds of hemorrhagic fever virus: hantavirus (HTNV), chikungunya fever virus (CHIKV), dengue virus (DENV), and Ebola virus (EBOV). It combined different rapid methods, including antibody-free enrichment of a specific virus, and LFB-based DNA detection. This assay may have potential for hemorrhagic fever virus detection in foods and other types of samples.

Conflicts of interest

The authors have declared that no conflict of interest exists.

Acknowledgements

This work was supported by Key Laboratory of Regenerative Biology, Guangzhou Institutes of Biomedicine and Health, Chinese Academy of Sciences, Stem Cell and Molecular Diagnostic Laboratory. This study was financially supported by the National Natural Science Foundation of China (31671933, to LZ), Guizhou Medical University Graduate Student Innovation Program (Guiyi YJSCXJH [2019] 001, to JZ).

Notes and references

1. G. Grard; Fair, J.N.; Lee, D.; Slikas, E.; Steffen, I.; Muyembe, J.J.; Sittler, T.; Veeraraghavan, N.; Ruby, J.G.; Wang, C.; Makuwa, M.; Mulembakani, P.; Tesh, R.B.; Mazet, J.; Rimoin, A.W.; Taylor, T.; Schneider, B.S.; Simmons, G.; Delwart, E.; Wolfe, N.D.; Chiu, C.Y.; Leroy, E.M., *PLoS pathogens* 2012, **8**, e1002924.

2. H. Li; Ying, T.; Yu, F.; Lu, L.; Jiang, S., *Microbes and infection /*

View Article Online
DOI: 10.1039/D0AY01137A

Institut Pasteur 2015, **17**, 109-17.

3. S.B. Rasheed; Butlin, R.K.; Boots, M., *Public health* 2013, **127**, 11-7.

4. W.K. Kim; No, J.S.; Lee, S.H.; Song, D.H.; Lee, D.; Kim, J.A.; Gu, S.H.; Park, S.; Jeong, S.T.; Kim, H.C.; Klein, T.A.; Wiley, M.R.; Palacios, G.; Song, J.W., *Emerging infectious diseases* 2018, **24**, 249-257.

5. L.C. Katzelnick; Fonville, J.M.; Gromowski, G.D.; Bustos Arriaga, J.; Green, A.; James, S.L.; Lau, L.; Montoya, M.; Wang, C.; VanBlargan, L.A.; Russell, C.A.; Thu, H.M.; Pierson, T.C.; Buchy, P.; Aaskov, J.G.; Munoz-Jordan, J.L.; Vasilakis, N.; Gibbons, R.V.; Tesh, R.B.; Osterhaus, A.D.; Fouchier, R.A.; Durbin, A.; Simmons, C.P.; Holmes, E.C.; Harris, E.; Whitehead, S.S.; Smith, D.J., *Science (New York, N.Y.)* 2015, **349**, 1338-43.

6. S.L. Badole; Yadav, P.D.; Patil, D.R.; Mourya, D.T., *Journal of vector borne diseases* 2015, **52**, 1-10.

7. H. Jiang; Du, H.; Wang, L.M.; Wang, P.Z.; Bai, X.F., *Frontiers in cellular and infection microbiology* 2016, **6**, 1.

8. F.J. Burt; Chen, W.; Miner, J.J.; Lenschow, D.J.; Merits, A.; Schnettler, E.; Kohl, A.; Rudd, P.A.; Taylor, A.; Herrero, L.J.; Zaid, A.; Ng, L.F.P.; Mahalingam, S., *The Lancet. Infectious diseases* 2017, **17**, e107-e117.

9. S. Bhatt; Gething, P.W.; Brady, O.J.; Messina, J.P.; Farlow, A.W.; Moyes, C.L.; Drake, J.M.; Brownstein, J.S.; Hoen, A.G.; Sankoh, O.; Myers, M.F.; George, D.B.; Jaenisch, T.; Wint, G.R.; Simmons, C.P.; Scott, T.W.; Farrar, J.J.; Hay, S.I., *Nature* 2013, **496**, 504-7.

10. R.A. Fowler; Fletcher, T.; Fischer, W.A., 2nd; Lamontagne, F.; Jacob, S.; Brett-Major, D.; Lawler, J.V.; Jacquerioz, F.A.; Houlihan, C.; O'Dempsey, T.; Ferri, M.; Adachi, T.; Lamah, M.C.; Bah, E.I.; Mayet, T.; Schieffelin, J.; McLellan, S.L.; Senga, M.; Kato, Y.; Clement, C.; Mardel, S.; Vallenas Bejar De Villar, R.C.; Shindo, N.; Bausch, D., *American journal of respiratory and critical care medicine* 2014, **190**, 733-7.

11. S. Safari; Baratloo, A.; Rouhipour, A.; Ghelichkhani, P.; Yousefifard, M., *Emergency (Tehran, Iran)* 2015, **3**, 3-7.

12. J.P. Xiao; He, J.F.; Deng, A.P.; Lin, H.L.; Song, T.; Peng, Z.Q.; Wu, X.C.; Liu, T.; Li, Z.H.; Rutherford, S.; Zeng, W.L.; Li, X.; Ma, W.J.; Zhang, Y.H., *Infectious diseases of poverty* 2016, **5**, 44.

13. Y.Z. Zhang; Zou, Y.; Fu, Z.F.; Plyusnin, A., *Emerging infectious diseases* 2010, **16**, 1195-203.

14. M. Mwanatambwe; Yamada, N.; Arai, S.; Shimizu-Suganuma, M.; Shichinohe, K.; Asano, G., *Journal of Nippon Medical School = Nippon Ika Daigaku zasshi* 2001, **68**, 370-5.

15. K.B. Laupland; Valiquette, L., *The Canadian journal of infectious diseases & medical microbiology = Journal canadien des maladies infectieuses et de la microbiologie medicale* 2014, **25**, 128-9.

16. T.E. Fletcher; Brooks, T.J.; Beeching, N.J., *BMJ (Clinical research ed.)* 2014, **349**, g5079.

17. L.J. Allen; Wesley, C.L.; Owen, R.D.; Goodin, D.G.; Koch, D.; Jonsson, C.B.; Chu, Y.K.; Shawn Hutchinson, J.M.; Paige, R.L., *Journal of theoretical biology* 2009, **260**, 510-22.

18. S. Arai; Taniguchi, S.; Aoki, K.; Yoshikawa, Y.; Kyuwa, S.; Tanaka-Taya, K.; Masangkay, J.S.; Omatsu, T.; Puentespina, R., Jr.; Watanabe, S.; Alviola, P.; Alvarez, J.; Eres, E.; Cosico, E.; Quibod, M.N.; Morikawa, S.; Yanagihara, R.; Oishi, K., *Infection, genetics and evolution : journal of molecular epidemiology and evolutionary genetics in infectious diseases* 2016, **45**, 26-32.

19. A.R. Salehuddin; Haslan, H.; Mamikutty, N.; Zaidun, N.H.; Azmi, M.F.; Senin, M.M.; Syed Ahmad Fuad, S.B.; Thent, Z.C., *Asian Pac J Trop Med* 2017, **10**, 211-219.

20. J.M. Jones; Schumacher, M.; Peoples, M.; Souders, N.; Horn, K.; Fox, L.; Scott, M.; Brady, S.; Weiss, J.; Komatsu, K.; Nieto, N., *MMWR. Morbidity and mortality weekly report* 2015, **64**, 651-2.

21. I.J. Schafer; Knudsen, E.; McNamara, L.A.; Agnihotri, S.; Rollin, P.E.; Islam, A., *The Journal of infectious diseases* 2016, **214**, S122-s136.

22. H. Gu; Leung, R.K.; Jing, Q.; Zhang, W.; Yang, Z.; Lu, J.; Hao, Y.; Zhang, D., *International journal of environmental research and public health* 2016, **13**.

23. H. Du; Wang, P.Z.; Li, J.; Bai, L.; Li, H.; Yu, H.T.; Jiang, W.; Zhang, Y.; Wang, J.N.; Bai, X.F., *BMC infectious diseases* 2014, **14**, 191.

24. L. Chen; Wei, H.; Guo, Y.; Cui, Z.; Zhang, Z.; Zhang, X.E., *Journal of immunological methods* 2009, **346**, 64-70.

25. T. Amada; Yoshimatsu, K.; Yasuda, S.P.; Shimizu, K.; Koma, T.; Hayashimoto, N.; Gamage, C.D.; Nishio, S.; Takakura, A.; Arikawa, J., *Journal of virological methods* 2013, **193**, 42-9.

26. L. Zoller; Yang, S.; Gott, P.; Bautz, E.K.; Darai, G., *Journal of medical virology* 1993, **39**, 200-7.

27. J.H. Kim; Chong, C.K.; Sinniah, M.; Sinnadurai, J.; Song, H.O.; Park, H., *Journal of clinical virology : the official publication of the Pan American Society for Clinical Virology* 2015, **65**, 11-9.

28. A. Diaz-Badillo; Munoz Mde, L.; Perez-Ramirez, G.; Altuzar,

View Article Online
DOI: 10.1039/D0AY01137A

V.; Burgueno, J.; Mendoza-Alvarez, J.G.; Martinez-Munoz, J.P.; Cisneros, A.; Navarrete-Espinosa, J.; Sanchez-Sinencio, F., *Sensors (Basel, Switzerland)* 2014, **14**, 7580-601.

29. G.T. Walker; Fraiser, M.S.; Schram, J.L.; Little, M.C.; Nadeau, J.G.; Malinowski, D.P., *Nucleic acids research* 1992, **20**, 1691-6.

30. Q. Guo; Yang, X.; Wang, K.; Tan, W.; Li, W.; Tang, H.; Li, H., *Nucleic acids research* 2009, **37**, e20.

31. Z. Fang; Wu, W.; Lu, X.; Zeng, L., *Biosensors & bioelectronics* 2014, **56**, 192-7.

32. M. Luo; Li, N.; Liu, Y.; Chen, C.; Xiang, X.; Ji, X.; He, Z., *Biosensors & bioelectronics* 2014, **55**, 318-323.

33. S. Li; Liu, S.; Xu, Y.; Zhang, R.; Zhao, Y.; Qu, X.; Wang, Y.; Huang, J.; Yu, J., *The Analyst* 2019, **144**, 4795-4802.

34. M. Komori; Komiya, K.; Shirakawa, T.; Morikawa, T.J.; Yoshimura, T., *Analytical and bioanalytical chemistry* 2019, **411**, 3789-3800.

35. J.-F. Huang; Zhao, N.; Xu, H.-Q.; Xia, H.; Wei, K.; Fu, W.-L.; Huang, Q., *Analytical and bioanalytical chemistry* 2016, **408**, 7437-7446.

36. S.F. Cheung; Cheng, S.K.L.; Kamei, D.T., *J Lab Autom* 2015, **20**, 316-333.

37. X. Lu; Liang, X.; Dong, J.; Fang, Z.; Zeng, L., *Analytical and bioanalytical chemistry* 2016, **408**, 6703-6709.

38. X. Huang; Zhai, C.; You, Q.; Chen, H., *Analytical and bioanalytical chemistry* 2014, **406**, 4243-4249.

39. J.H. Leuvering; Thal, P.J.; Van der Waart, M.; Schuurs, A.H., *Journal of immunological methods* 1981, **45**, 183-194.

40. S. Nishat; Awan, F.R.; Bajwa, S.Z., *Analytical sciences : the international journal of the Japan Society for Analytical Chemistry* 2019, **35**, 123-131.

41. X. Li; Lu, D.; Sheng, Z.; Chen, K.; Guo, X.; Jin, M.; Han, H., *Talanta* 2012, **100**, 1-6.

42. Y. Maheshwari; Vijayanandraj, S.; Jain, R.K.; Mandal, B., *Journal of virological methods* 2018, **253**, 43-48.

43. M.J. Raeisossadati; Danesh, N.M.; Borna, F.; Gholamzad, M.; Ramezani, M.; Abnous, K.; Taghdisi, S.M., *Biosensors & bioelectronics* 2016, **86**, 235-246.

44. J.W.-F. Law; Ab Mutalib, N.-S.; Chan, K.-G.; Lee, L.-H., *Frontiers in microbiology* 2015, **5**, 770-770.